Cancer Immunology, Immunotherapy (submitted in 2023) – Yan Luo et al.
Supplementary Figures

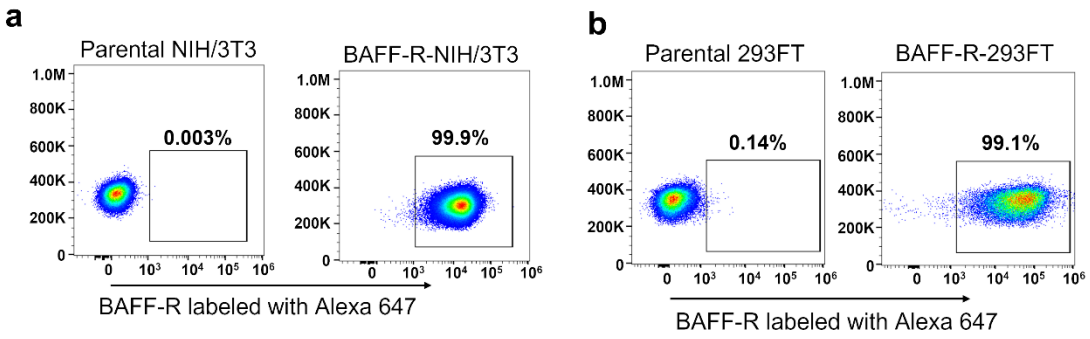

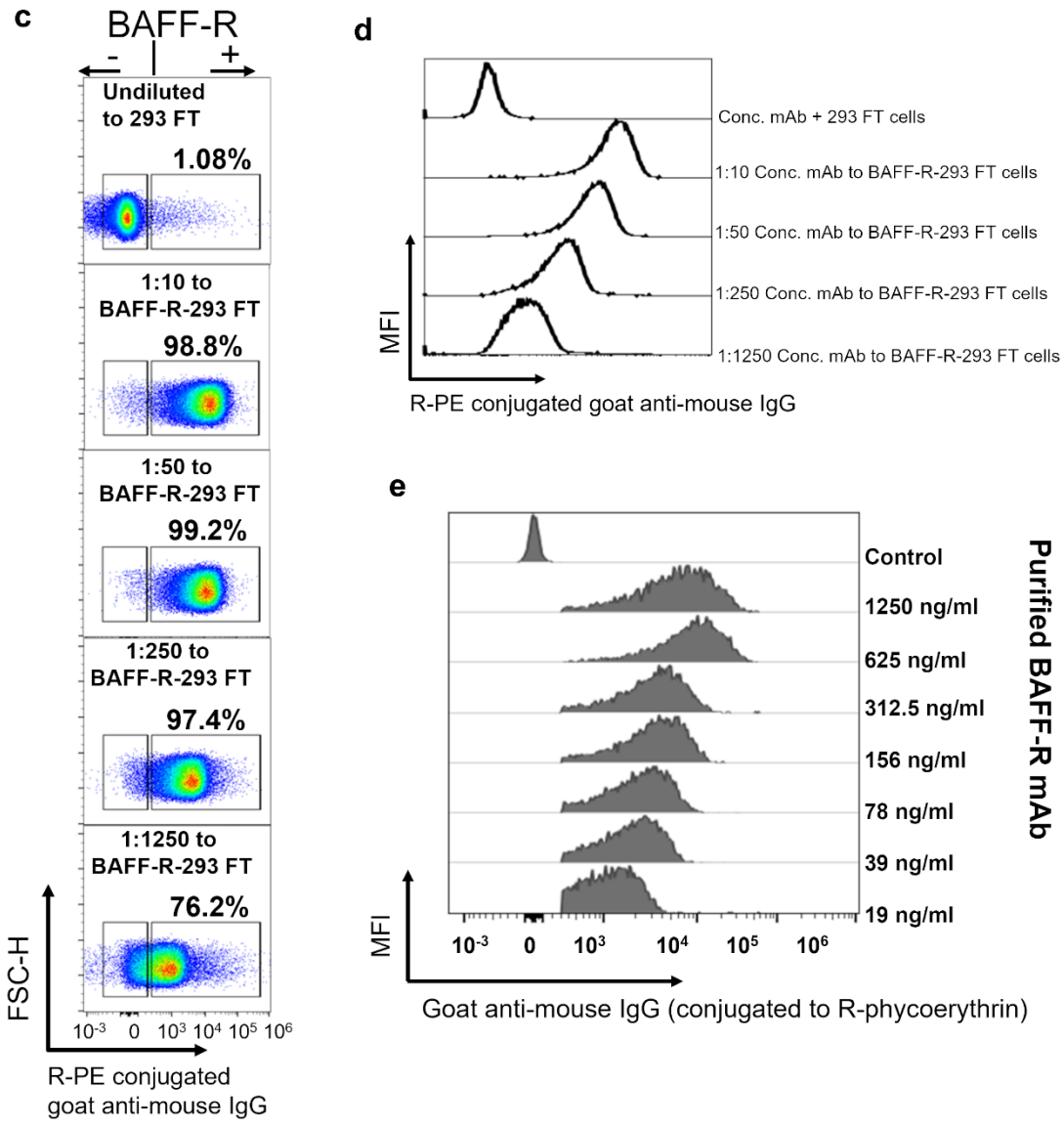

Supplementary Fig. 1 Generation of a novel anti-BAFF-R antibody. BAFF-R-pCDH (pCDH cDNA Cloning and Expression Lentivectors, System Biosciences, Palo Alto, CA.) lentivirus infected NIH/3T3 or 293FT cells were selected with 1 μg/mL puromycin (Sigma-Aldrich, St. Louis, MO, USA) for 1 week; single-cell clones were established from sorted BAFF-R positive NIH/3T3 or BAFF-R positive 293FT cells, and a BAFF-R expressing NIH/3T3 cell clone were used as the immunogen for BAFF-R monoclonal antibody development. The expression of BAFF-R in a BAFF-R-NIH/3T3 single-cell clone (**a**) or a BAFF-R-293FT cell line (**b**) was confirmed by flow cytometry. **c.** Crude C21 hybridoma supernatants were screened for antigen specific binding using BAFF-R-positive and BAFF-R-negative 293FT cells with a 5-fold serial diluted concentration to generate this representative data. **d.** The antigen specific binding was detected with R-PE conjugated goat anti-mouse IgG for 30 mins at 4^{o}C. **e.** Antigen specific binding affinity of purified mAb C21 with serial diluted concentration (from 19 ng/ml to 1250 ng/ml) to BAFF-R-positive and BAFF-R-negative 293FT cells.

a

b

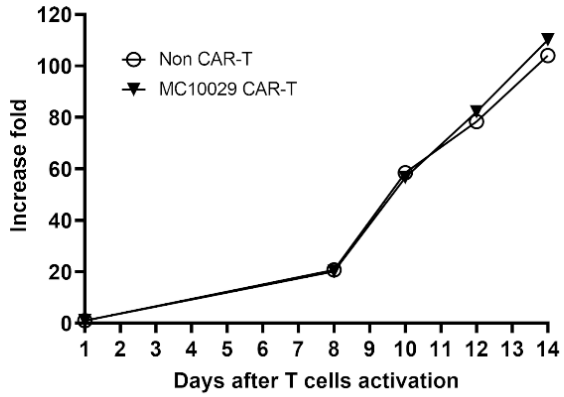

c

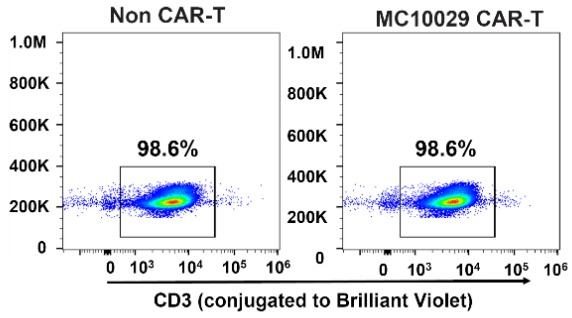

d

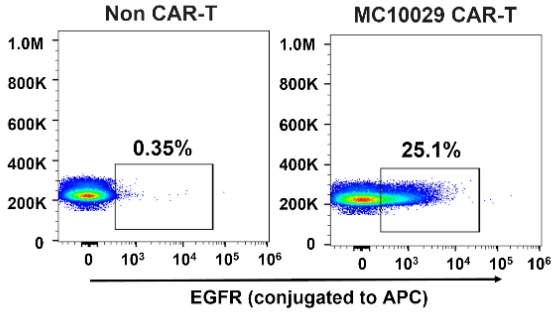

e

	Production 1		Production 2		Production 3	
	Non CAR-T	MC10029 CAR-T	Non CAR-T	MC10029 CAR-T	Non CAR-T	MC10029 CAR-T
Fold expansion	87.2	82.6	76.5	72.6	82.3	90.2
Viability(%)≥70%@D14	92	94	89	88	91	93
Identity(%) ≥80%	99.0	98.7	99.7	99.8	97.9	98.3
Potency(%) ≥10%	0.18	23.9	0.34	22.6	0.34	21.7

Supplementary Fig. 2 MC10029 CAR construct and initial characterization of MC10029 CAR-T cells production. a. Schematic diagram the functional elements within the CAR design. The construct included the following elements in tandem: signal peptide (SP); the scFv of our novel BAFF-R antibody; a IgG4 hinge; CD28 transmembrane (TM) domain; CD28 costimulatory domain (CD28QQ); CD3ζ; T2A (self-cleaving 2A peptide); and tEGFR (truncated epidermal growth factor receptor). **b.** Fold expansion of CAR-T cells was calculated from day 1 to day 14 by measuring the number of viable CAR-T cells by trypan blue exclusion using Bio-Rad Cell counter. Non CAR-T cells from the same donor were used as controls. **c,d.** MC10029 CAR-T cells were stained with antibodies to measure surface expression of CD3 for identity (**c**) or EGFR for potency (**d**) to characterize the CAR-T cells with the data shown in these representative flow cytometry dot plots. Non CAR-T cells from the same donor were used as controls. **e.** These characterization assays were performed on three production batches of MC10029 CAR - T cells that were used in various in vitro assays. Each batch of CAR-T cells destined for research testing were evaluated for cell quality with Fold Expansion (> 25) and Viability (> 70%, as determined by Trypan Blue staining) as well as CAR-T cell specific characterization with Identity (> 80%, as determined by flow cytometry for CD3 positive cells) and Potency (> 10%, as determined by flow cytometry for EGFR positive T cells). EFGR is a transgene that is accepted as a measure of potency, per guidance documents for CAR-T cell product development.

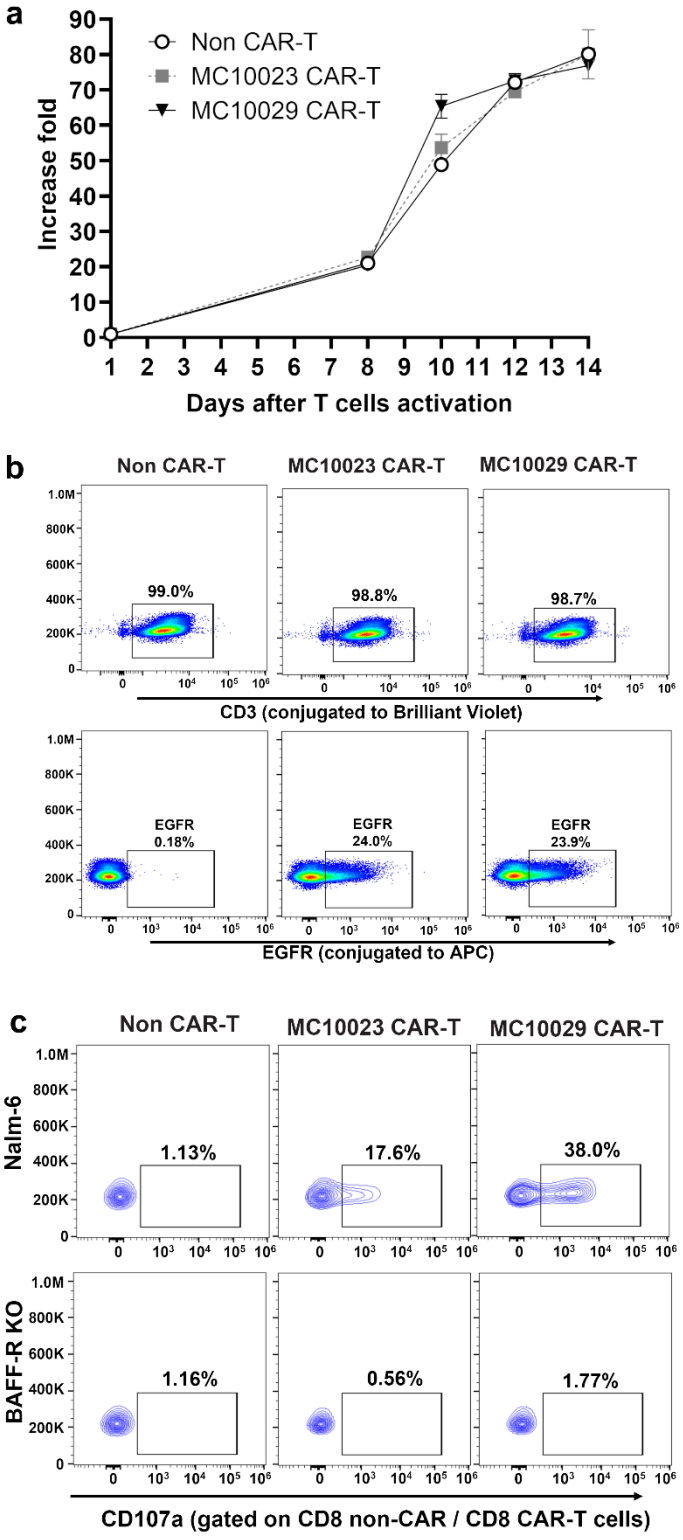
a
Non CAR-T
MC10023 CAR-T
MC10029 CAR-T
Increase fold
Days after T cells activation
b
Non CAR-T
MC10023 CAR-T
MC10029 CAR-T
99.0%
98.8%
98.7%
CD3 (conjugated to Brilliant Violet)
EGFR 0.18%
EGFR 24.0%
EGFR 23.9%
EGFR (conjugated to APC)
c
Non CAR-T
MC10023 CAR-T
MC10029 CAR-T
Nalm-6
1.13%
17.6%
38.0%
Nalm-6 BAFF-R KO
1.16%
0.56%
1.77%
CD107a (gated on CD8 non-CAR / CD8 CAR-T cells)

Supplementary Fig. 3 Comparison of BAFF-R CAR-T cell constructs with differing costimulatory domains. With the option of complementing CD3ζ with either the CD28 costimulatory domain (MC10029) or the 4-1 BB costimulatory domain (MC10023), both CARs were generated and transduced into T cells to identify which BAFF-R CAR-T cells provided superior antigen specific cytotoxicity. **a**. Expansion of MC10023 and MC10029 CAR-T cells showed comparable fold increases by day 14. **b.** The T cell content (CD3) and the proportion of CAR-T cells (using EGFR as a proxy) within the final products of both MC10029 and MC10023 CAR-T cells are also found to be comparable. **c.** Antigen specific cytotoxicity was assayed by testing MC10023 CAR-T cells or MC10029 CAR-T cells against Nalm-6 and Nalm-6 BAFF-R KO cell lines; this degranulation assay shows the higher activity of MC10029 CAR-T cells compared to MC10023 CAR-T cells and justified the advancement of MC10029 CAR-T cells into our other experiments.

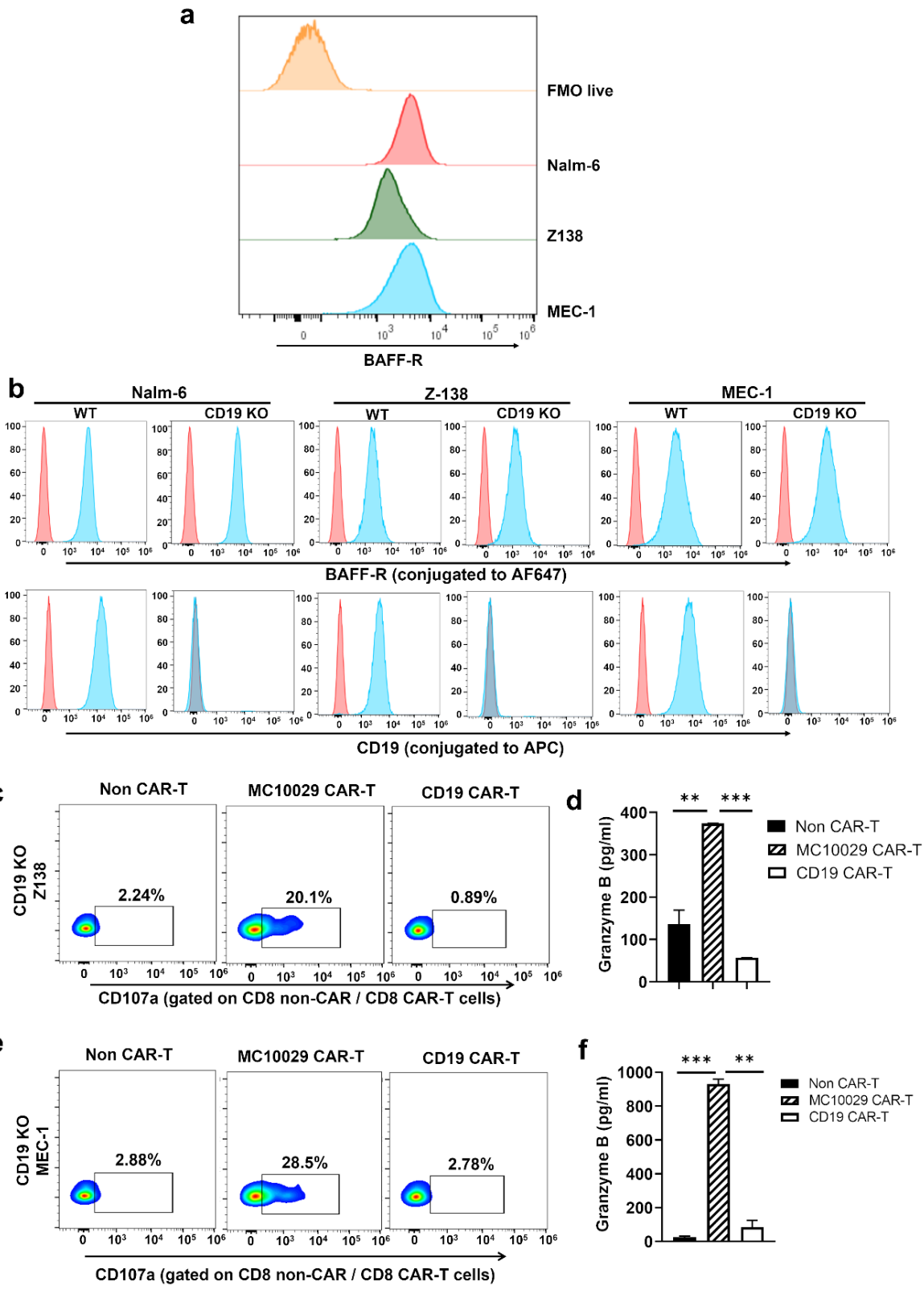
a
FMO live
Nalm-6
Z138
MEC-1
BAFF-R
b
Nalm-6
Z-138
MEC-1
WT
CD19 KO
BAFF-R (conjugated to AF647)
CD19 (conjugated to APC)
c
Non CAR-T
MC10029 CAR-T
CD19 CAR-T
CD19 KO Z138
2.24%
20.1%
0.89%
CD107a (gated on CD8 non-CAR / CD8 CAR-T cells)
d
Granzyme B (pg/ml)
**
***
Non CAR-T
MC10029 CAR-T
CD19 CAR-T
e
CD19 KO MEC-1
2.88%
28.5%
2.78%
CD107a (gated on CD8 non-CAR / CD8 CAR-T cells)
f
Granzyme B (pg/ml)
***
**

Supplementary Fig. 4 In vitro cytotoxicity of MC10029 CAR-T cells against CD-19 deficient malignant B-cell tumor lines. Three cell lines that are used to evaluate cytotoxicity of MC10029 CAR-T cells were tested for antigen expression. **a.** Using anti-BAFF-R-AF647 antibody, flow cytometry histograms show BAFF-R expression in Nalm-6, Z-138, or MEC-1. **b.** These cell lines were also evaluated for CD19 surface expression using anti-CD19-APC antibody. CD19 knock-out (KO) Nalm-6, Z-138, and MEC-1 variants were generated and evaluated for antigen surface expression. Flow cytometry histograms show BAFF-R expression in wild type Nalm-6, Z-138, or MEC-1 cell lines, as well as their CD19-deficient counterparts. **c, e.** Flow cytometry plots show the functional potency of CAR-T cells against CD19-deficient tumor cells by the surface expression CD107a in a degranulation assay. Non-CAR-T cells, MC10029 CAR-T cells, or CD19 CAR-T cells were generated from the same donor and incubated with CD19-deficient Z-138 (**c**) or CD19-deficient MEC-1 (**e**) cells at an E:T ratio of 2:1 to characterize the cytotoxicity of MC10029 CAR-T cells against these CD19-deficient tumor cells. **d, f.** Granzyme B ELISA shows functional potency of MC10029 CAR-T cells against CD19-deficient tumor cells. Non-CAR-T cells, MC10029 CAR-T cells, or CD19 CAR-T cells were co-incubated with CD19-deficient Z-138 (**d**) or CD19-deficient MEC-1 (**f**) cells at an E:T ratio of 4:1 for 72 hours when the supernatants were harvested for subsequent ELISA. Graphed data are means of quadruplicate sampling. The data are representative of three independent experiments.

a

Identifier	Disease	Gender	Age (Years)
1	B-CLL	Female	77
2	B-CLL	Male	63
3	B-CLL	Female	83
4	B-CLL	Male	78
5	B-CLL	Female	65
6	B-CLL	Male	56
7	B-CLL	Male	77
8	B-CLL	Male	64
9	B-CLL	Female	54

b

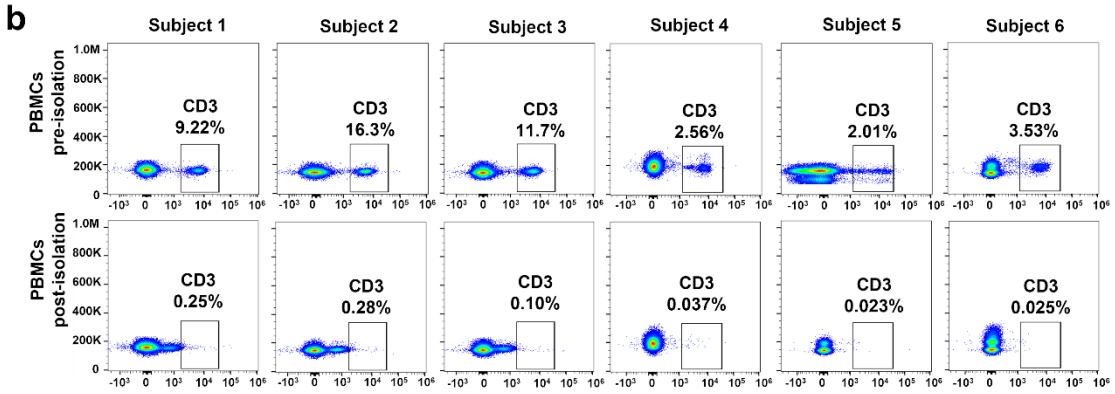

c

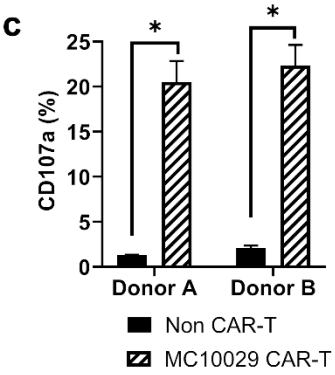

d

	Subject 2		Subject 3		Subject 4		Subject 5	
	Non CAR-T	CAR-T[1]	Non CAR-T	CAR-T[1]	Non CAR-T	CAR-T[1]	Non CAR-T	CAR-T[1]
Granzyme A								
pg/ml	518	**2037****	1169	**3656****	572	**3898****	320	**1980****
Fold change[2]	1	**5.7**	1	**3.1**	1	**6.8**	1	**6.2**
Perforin								
pg/ml	452	**1413****	677	**1593****	1056	**3066****	549	**1792****
Fold change[2]	1	**3.1**	1	**2.4**	1	**2.9**	1	**3.3**
IFN-γ								
pg/ml	3102	**4683****	1416	**3577****	565	**1336****	146	**457****
Fold change[2]	1	**1.5**	1	**2.5**	1	**2.4**	1	**3.1**

[1] CAR-T = MC10029 CAR-T cells
[2] Fold change is calculated by dividing pg/ml from MC10029 CAR T-cells by those from non-CAR T-cells.

Supplementary Fig. 5 Supporting data on the activity of MC10029 CAR-T cells against primary CLL tumor cells. a. Basic demographic data for the nine B-CLL subjects evaluated with MC10029 CAR-T cells. **b.** Subject PBMCs were enriched for CLL tumor cells, and the removal of endogenous T cells was confirmed in these six samples by characterizing the CD3 positive T cells in the original PBMC samples (top panels) and enriched B cell population (bottom panels). **c.** Statistical analysis of degranulation data in **Fig. 4d** shows statistical significance in cytotoxicity against primary CLL tumor cells between MC10029 CAR-T cells and Non CAR-T cells ($* p < 0.05$), while no difference was noted between Donor A and Donor B. **d.** Release of multiple granule proteins/cytokines from MC10029 CAR-T cells incubated with primary CLL tumor cells isolated from selected subjects. There was a significant increase observed in the release of granule proteins in CAR-T cell groups compared to the Non CAR-T cell groups. ($**p<0.01$)

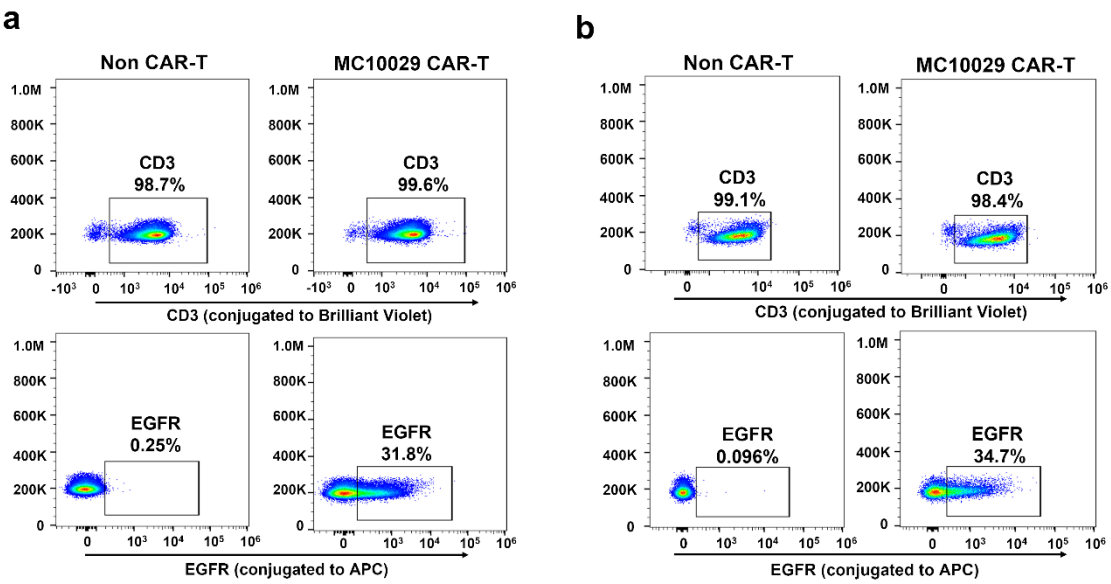

c

	Healthy donor A		Healthy donor B	
	Non CAR-T	MC10029 CAR-T	Non CAR-T	MC10029 CAR-T
Fold expansion	82.5	79.5	59.7	55.7
Viability(%) ≥ 70%@D13	84	78	82	81
Identity(%) ≥ 80%	98.7	99.6	99.1	98.4
Potency(%) ≥ 10%	0.25	31.8	0.096	34.7

Supplementary Fig. 6 Characterization of MC10029 CAR-T cells used in the experiments shown in Figure 4. MC10029 CAR-T cells were generated from two healthy donors and tested against primary CLL tumor cells. The two production batches of MC10029 CAR-T cells were characterized using our standard QC assays. The identity (CD3 positive cells) and the potency (EGFR positive cells) of MC10029 CAR-T cells from donor A (**a**) were nearly identical as those from donor B (**b**). (**c**) Both batches of MC10029 CAR-T cells met our requirements in terms of QC parameters, including fold expansion, viability, identity, and potency.

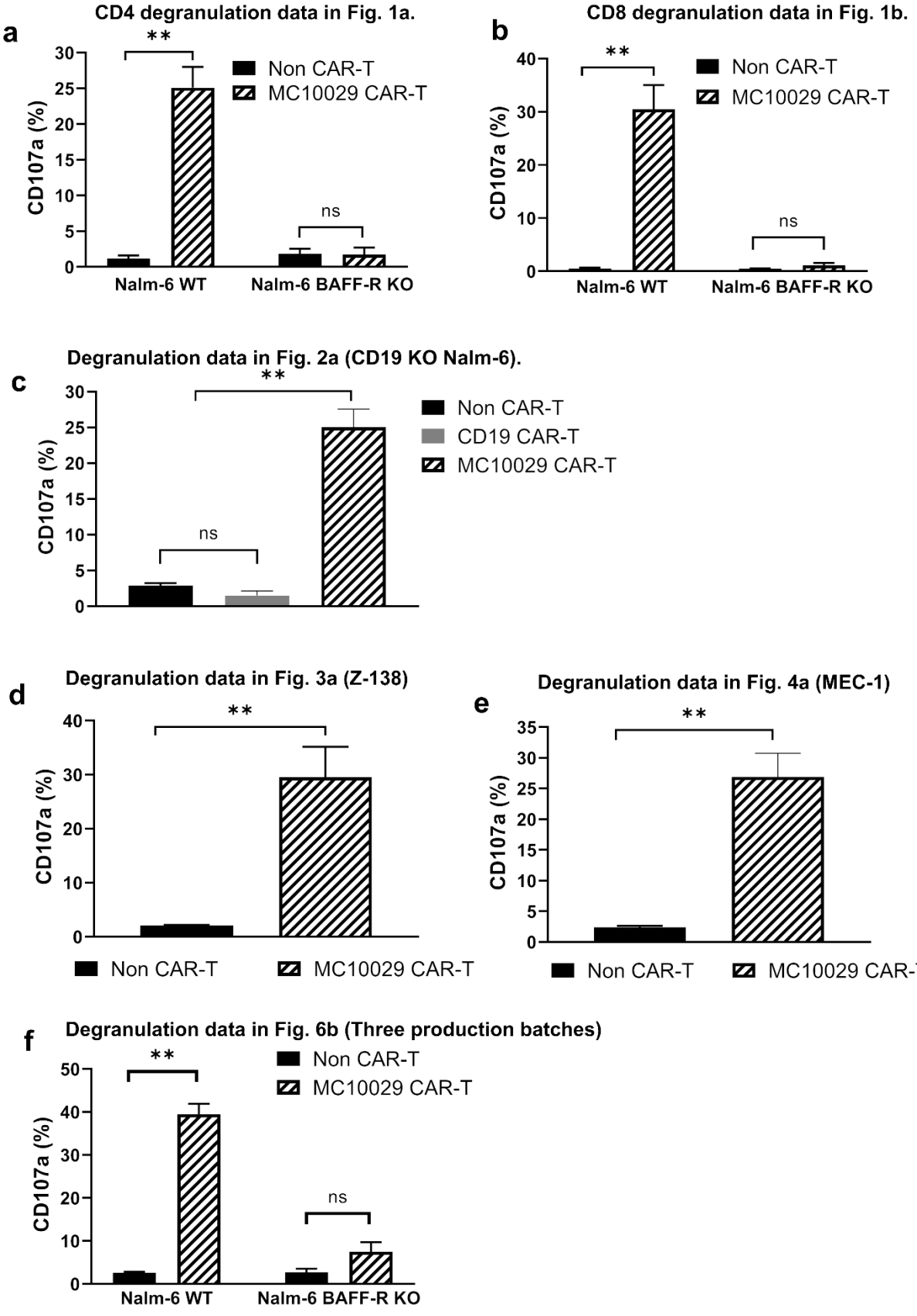
a
CD4 degranulation data in Fig. 1a.
**
ns
Non CAR-T
MC10029 CAR-T
CD107a (%)
Nalm-6 WT
Nalm-6 BAFF-R KO
b
CD8 degranulation data in Fig. 1b.
**
ns
Non CAR-T
MC10029 CAR-T
CD107a (%)
Nalm-6 WT
Nalm-6 BAFF-R KO
c
Degranulation data in Fig. 2a (CD19 KO Nalm-6).
**
ns
Non CAR-T
CD19 CAR-T
MC10029 CAR-T
CD107a (%)
d
Degranulation data in Fig. 3a (Z-138)
**
CD107a (%)
Non CAR-T
MC10029 CAR-T
e
Degranulation data in Fig. 4a (MEC-1)
**
CD107a (%)
Non CAR-T
MC10029 CAR-T
f
Degranulation data in Fig. 6b (Three production batches)
**
ns
Non CAR-T
MC10029 CAR-T
CD107a (%)
Nalm-6 WT
Nalm-6 BAFF-R KO

Supplementary Fig. 7 Statistical analysis of CD107a degranulation assays. a. Statistical analysis of degranulation data of MC10029 CD4 CAR-T cells in Fig. 1a. **b.** Statistical analysis of degranulation data of MC10029 CD8 CAR-T cells in Fig. 1b. **c.** Statistical analysis of degranulation data of MC10029 CAR-T cells against CD19 KO Nalm-6 cells in Fig. 2a. **d.** Statistical analysis of degranulation data of MC10029 CAR-T cells against Z-138 cells in Fig. 3a. **e.** Statistical analysis of degranulation data of MC10029 CAR-T cells against MEC-1 cells in Fig. 4a. **f.** Statistical analysis of degranulation data of three production batches of MC10029 CAR-T cells in Fig. 6b. (** $p < 0.01$; ns: no significance)